Progress in Chemical and Biochemical Research

Journal homepage: www.pcbiochemres.com

Original Research Article

Disinfection by-Products Removal Evaluation from Aqueous Solution by Hybrid Filtration Process

Mohsen Vaziri, Seyed Mostafa Tabatabaee Ghomsheh*, Alireza Azimi, Masoumeh Mirzaei

Department of Chemical Engineering, Mahshahr Branch, Islamic Azad University, Mahshahr, Iran

ARTICLE INFO

Article history

Submitted: 2020-01-29
Revised: 2020-06-04
Accepted: 2020-07-16
Available online: 2020-09-10
Manuscript ID: PCBR-2007-1116
DOI: 10.22034/pcbr.2020.113923

KEYWORDS

Adsorption
Haloacetonitrile
Membrane
Nanofiltration

ABSTRACT

In this study removal of haloacetonitriles from aqueous solution by employing a novel hybrid filtration process is investigated. The application potential of the oxidized multi-walled carbon nanotubes (O-MWCNTs) as adsorbent was investigated by evaluating the effect of different process parameters. Solution pH significantly affected the removal of DCAN (as a model of HANs) due to its strong effect on the charges of the adsorbent and the adsorbate. A maximum DOC removal of 98.7% for was achieved with 150 mg/L oxidized MWCNTs dosage and at a solution pH of 8. Finally, the nanofiltration technique using a PBS membrane was effectively employed to reject the wastewater pollutants (HANs) proprly.

GRAPHICAL ABSTRACT

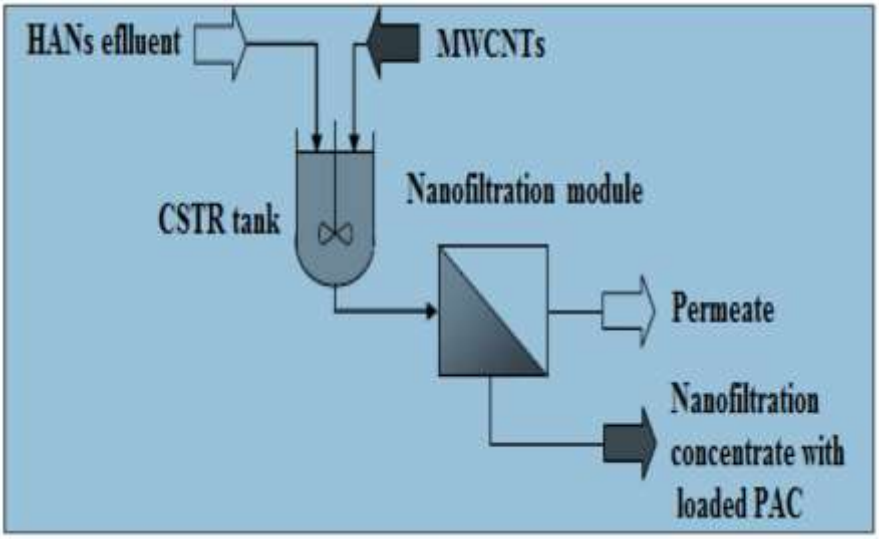

* Corresponding author: Seyed Mostafa Tabatabaee Ghomsheh
✉ E-mail: : Mostafa.tabatabaee@yahoo.com

INTRODUCTION

The haloacetonitriles (HANs) are of the compounds that exist in drinking water exclusively as byproducts of disinfection. These compounds arise when surface water is treated by chloramination. Human exposure occurs through consumption of finished drinking water; oral and dermal contact also occurs, and results from showering, swimming and other activities [1]. The disinfection of drinking water reduces microbial risks but increases chemical exposure to man. Increasing of human health risks are due to the formation of disinfection by-products (DBPs) in the organic and inorganic precursors [2]. Common HANs generated during the disinfection process consist of dichloroacetonitrile, (BCAN) bromochloroacetonitrile, dibromoacetonitrile and (TCAN) trichloroacetonitrile. Due to their potential health effects, the World Health Organization has suggested guideline values of 20 μg L^{-1} for DCAN, 70 μg L^{-1} for DBAN and 1 μg L^{-1} for TCAN [3]. Due to their high cytotoxicity and genotoxicity require more consideration, so various processes, such as adsorption [4-7], membrane filtration [8-10] and ozonation [11-13] have been employed to remove the disinfection by-products (DBPs) from water. Membrane separation process is being emerged as an innovative wastewater treatment technology. However, its use at present is limited due to its high cost of installation and its long-term operational difficulty.The membrane processes such as Micro or Ultrafiltration is a cost-effective option, but they cannot remove dissolved organic matter due to their relatively larger pore sizes [14].

Recently, among membrane technology nanofiltration and reverse osmosis have attracted a great deal of attention for use in water softening and the removal of various contaminants from drinking-water sources. But these technologies have inherent drawbacks: lower permeate flux in nanofiltration and higher transmembrane pressure in reverse osmosis, thus lower process efficiency and higher cost of investment and operation. Recently, hybrid membrane filtration systems are used as an alternative way to achieve a high removal efficiency of organic matter in a cost-effective manner [15]. For example, double membrane processes combining porous membranes with reverse osmosis followed by advanced oxidation represent the state of the art in advanced water treatment for high-quality water reuse. Although very effective for the elimination of the contaminants, the double membrane process is associated with high capital and operating cost, and involves the use of chlorinated chemicals to suppress membrane fouling. Furthermore, cost-efficient methods for the treatment of RO concentrate containing salts, nutrients, disinfection by-products and micropollutants are not yet available. Against this backdrop, nanofiltration provides an interesting alternative to reverse osmosis with a number of advantages in particular less problematic membrane concentrates [16-18].

The lower operating pressure leads to reduced energy demands of 0.6 - 1.2 kWh/m^3 compared to 1.5 - 2.5 kWh/m^3 with RO. To achieve a comparable removal of pollutants, nanofiltration has to be combined with additional separation processes such as adsorption to activated carbon [19].

To the best of our knowledge, the removal of HANs from aqueous solution by adsorption- nanofiltration hybrid process has not been investigated. For a better understanding of the adsorption mechanism, the equilibrium data were fitted with adsorption isotherm models, and the kinetic parameters were calculated to determine the likely adsorption mechanism. In addition, the effect of the solution pH and the selective adsorption of five different HAN compounds differing in halogen groups or numbers were investigated as single and mixed solutes. Finally, the effect of oxidized MWCNTs on poly (butylene succinate) (PBS) membrane performance, especially on removal rates of HANs by oxidized MWCNTs-NF process and improvement of membrane flux are investigated [20].

MATERIALS AND METHOD

Commercial standards including mono-chloroacetonitrile (MCAN), monobromoacetonitrile (MBAN), dichloroacetonitrile (DCAN), dibromoacetonitrile (DBAN), trichloroacetonitrile (TCAN) were purchased from Aldrich. Commercial

MWCNTs were purchased from Hanwha nanotech (*MWCNT* CM-95, Korea). Other chemicals used in this study were of analytical grade and were procured from Merck, India. Distilled water was used throughout for solution preparations.

Preparation and characterization of biodegradable PBS membrane

Asymmetric flat sheet membrane of PBS was prepared using phase inversion method induced by immersion precipitation. At first, PBS was dissolved in 1-methyl-2 pyrrolidone (NMP) while concentration of total polymer was adjusted to be 17 %. The solution was stirred at 50 ^{o}C continuously till completely transparent mixture was obtained. After degassing, the casting solution was subsequently poured onto a glass plate, and spread with a membrane applicator to be as thin as 250 μm. Then, the glass plate was immediately immersed in distilled water bath at temperature of 50 ^{o}C for immersion precipitation. Finally, the membrane was dried using vacuum oven at 40 ^{o}C [20, 21]. Detailed properties of the PBS membrane are presented in **Table 1**.

Table 1. Properties of prepared PBS membrane.

Property	Value
Porosity (%)	45
Contact angle(^{o})	76
Pure water permeability (Lm^{-2} $h^{-1}bar^{-1}$)	18.3
Average pore size(nm)	43
Tensile strength (MPa)	53.2

Oxidation of MWCNTs

For oxidation of MWCNTs, at fist 2 g MWCNTs were placed in a flask and 300 ml nitric acid (65%) was added. The mixture was stirred for 48 hours at 120° C and then cooled up to ambient temperature. After that this mixture diluted with 500 ml DI water and vacuum-filtered through filter paper. Until the pH became neutral washing was continued, followed by drying in a vacuum oven at 100℃.

Process Design

Figure 1 presents the schematic of the MWCNTs/NF process. O-multi-walled carbon nanotubes is dosed to water sample including HANs molecules in a completely stirred tank reactor (CSTR). The suspension is then fed to the crossflow loop of a nanofiltration unit. The PBS membrane was used for solute rejection analyzing with an effective filtration area of 52.24 cm^2. The membrane was operated in crossflow mode with a crossflow velocity of 1.2 m/s and a recovery of 75%. Backflush with permeate was applied for 1 min every 45 min. Contact time in the O-MWCNTs reactor was 1 h. In order to develop a hybrid process for HANs removal, following the adsorption process nanofiltration technique was incorporated instead of the conventional centrifugal filtration. The permeate flux was measured at applied pressure of 7 bars by calculating the time required for collecting 20 mL permeate solution. The collected permeate solution was subsequently analyzed for residual HAN concentration in terms of DOC and ultraviolet absorbance at 254 nm (UV254). DOC was analyzed in a TOC analyzer (Shimadzu TOC-VCPN). UV absorbance was measured in an UV–visible spectrophotometer.

The supernatant solution was analyzed by gas chromatography equipped with electron capture detector (GC/ECD) according to EPA method 551.1, each experiment was performed in triplicate under identical conditions.

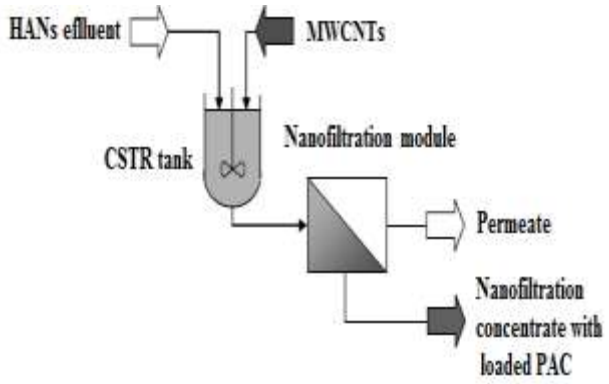

Fig. 1. Schematic of the O-MWCNTs/NF Process

Adsorption Study

All experiments to study HANs adsorption using O-MWCNTs were carried out at ambient temperature (~25 °C). for this purpose, 0.025 gr of O-MWCNTs was added in water sample (30 ml) and stirred for 1 min rapid mixing at 100 rpm and 30 min slow mixing at 30 rpm, and the ionic strength IS being fixed at 10 m mol L^{-1} using phosphate buffer. Then water sample was filtrated by a 0.45 µm filter.

HANs adsorption (%) at any instant of time was determined by the following equation:

$$HANs\ adsorption\ (\%) = \frac{C_f - C_p}{C_f} \times 100$$

Where, C_f and C_p are the concentrations of HANs at the initial time and at time t (µg L^{-1}) respectively. The amount of HAN sorbed (µg HAN/g adsorbent) was calculated by the following mass balance equation, and expressed as adsorption uptake (q):

$$q\left(\frac{mg}{g}\right) = \frac{(C_f - C_p)V}{m}$$

Where, V is the volume of HAN containing solution and m is the mass (g) of adsorbent.

Adsorption isotherms and kinetics

In order to elucidate the mechanism of adsorption and the potential rate controlling steps of processes such as mass transport and chemical reaction, kinetic models were applied to examine the experimental data [23]. These included pseudo-first order, pseudo-second order and intraparticle diffusion models.

The pseudo first order model can be described as follows:

$$\ln(q_e - q_t) = lnq_e - k_1 t$$

The pseudo-second order kinetic rate equation is expressed as:

$$\frac{t}{q_t} = \frac{1}{k_2 {q_e}^2} + \frac{t}{q_e}$$

The Intraparticle diffusion model given by:

$$q_t = k_d t^{1/2} + C$$

In these equations k_1 (min^{-1}), k_2 (g µg^{-1} min^{-1}) and k_d (µg g^{-1} $min^{-1/2}$) are the rate constants of pseudo-first order, pseudo-second order and intraparticle diffusion models. q_e, q_t (µg g^{-1}) are the adsorption uptake at equilibrium and at time t (min). C in Intraparticle diffusion model is a constant relating to the boundary layer thickness.

The distribution of HANs between the liquid and solid phases can be described by isotherm models such as those of Langmuir and Freundlich. These models describe how the amount of a substance adsorbed onto a surface depends on its pressure (if a gas) or its concentration (if in a solution), at a constant temperature.

The Langmuir model assumes that the adsorption of adsorbate occurs on a homogenous surface by monolayer adsorption without any interaction between adsorbed particles. The Langmuir adsorption isotherm is expressed by following equation:

$$q_e = \frac{q_m . K_L . C_e}{1 + K_L C_e}$$

Where q_m is the maximum adsorption capacity (µg g^{-1}) and K_L is the Langmuir constant.

The Freundlich model assumes that the adsorption of adsorbate occurs on a heterogeneous surface by monolayer adsorption. This empirical equation takes the form:

$$q_e = K_F {C_e}^{1/n}$$

Where K_F and n are the Freundlich constants.

RESULT AND DISCUSSION

FTIR Analysis of O-MWCNTs

Figure 2 shows the FTIR spectrum of oxidized MWCNTs. this Fig indicates that the acid treatment process introduces new functional

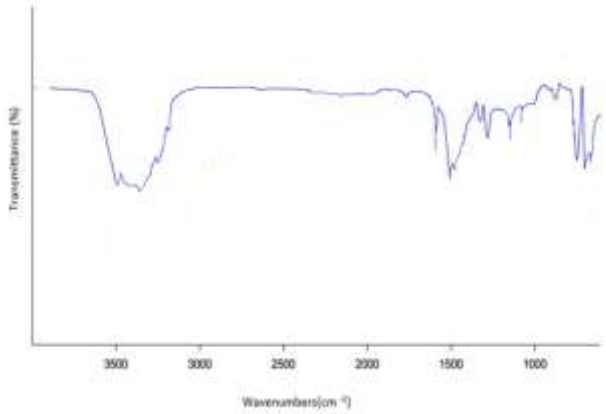

Fig. 2. FTIR spectrum of oxidized MWCNTs

The peak at 3462cm^{-1}, 1534cm^{-1}, and 1611 cm^{-1} is attributed to the hydroxyl groups, carboxyl groups and carbonyl groups.

A large number of chemical adsorption sites created on the surface by these functional groups and thereby the adsorption capacity can be increased. (**Fig. 3**).

Sorption Experiment

In any adsorption process adsorbent dosage and solution pH influence the adsorbate removal. Hence, the effects of these parameters were examined in detail for HANs.

Effect of adsorbent dosage on the adsorption of HANs

Fig. 3 presents the effect of O-MWCNTs dosage on the adsorption of HANs molecules. It can be seen from the figure that an increase in the O-MWCNTs amount more than 150 mg/L, increased the percentage sorption and decreased adsorption uptake. This is can be due to an increase in the number of active sites with an increase in the adsorbent amount. On the other hand, decrease in the adsorption uptake is due to unsaturated sites on the O-MWCNTs at a high dosage. A maximum uptake of HANs molecules was obtained using 150 mg/L of the adsorbent.

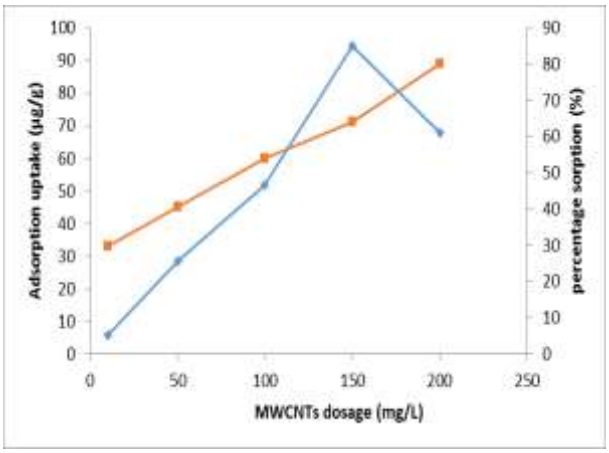

Fig. 3. Effect of O-MWCNTs dosage on the adsorption of HANs

Effect of pH on DCAN adsorption

The effect of solution pH on DCAN adsorption by O-MWCNTs is shown in **Fig. 4**. It reveals that the percentage sorption of DCAN is high at the solution pH from 7 to 9 and the removal increased with an increase in the solution pH up to 7. The maximum DCAN removal was observed at PH 8. The DCAN gives positively charged ions when dissolved in water. O-MWCNTs had a more negatively charged surface at pH 9 which was electrically attracted by a high positive dipole of the H atom in the DCAN molecules. . At pH<7 the positively charged surface of sorbent tends to oppose the adsorption of the cationic adsorbate.

When pH of DCAN solution is increased the surface acquires a negative charge, there by resulting in an increased adsorption of DCAN due to an increase in the electrostatic attraction between positively charged DCAN and negatively charged adsorbent.

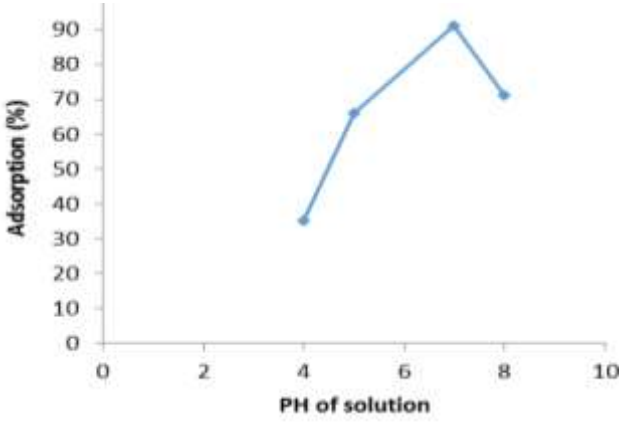

Fig. 4. Effect of solution pH on DCAN adsorption

O-MWCNTs had a more negatively charged surface at pH 9 which was electrically attracted by a high positive dipole of the H atom in the DCAN molecules.

Selective Adsorption of HANs in Solution

Results show that due to the high molecular weight of tri-HAN and di-HANs, they could have been more easily adsorbed than the smaller mono-HANs, and the strength of the positive dipole of di-HANs enhanced the adsorption capacity via ion–dipole electrostatic interactions. So in the single-solute solution, the order of adsorption preference on O-MWCNTs was DBAN > DCAN > TCAN≅ MBAN≅ MCAN (**Fig. 5a**).

The adsorption capacity of each HAN in the mixed solute solution on O-MWCNTs was slightly less than that in the single-solute solution. Generally, the sorption of the organic solute was dominated by the surface adsorption at low concentrations, and the organic partition dominated at high adsorbate concentration. Since the overall concentration in mixed HANs solution is high, so the obviously decreased adsorption capacity of each HAN is taken Due to segregation of active sites for HAN5 (**Fig.5b**).

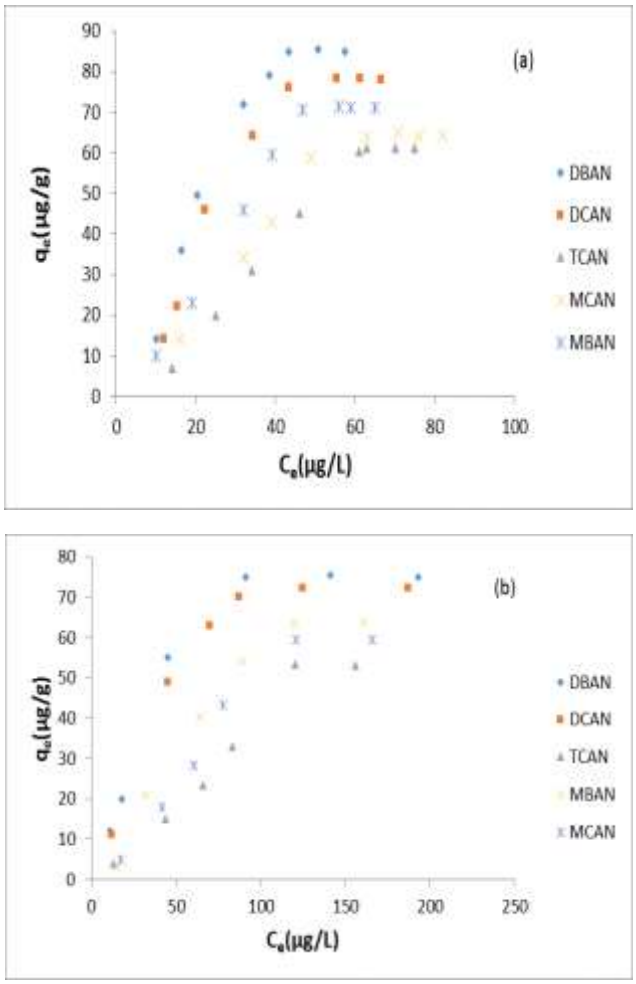

Fig. 5. Adsorption isotherms of HANs (at :pH= 8, IS= 10 mmol L^{-1}, and T =25°C)
a) in a single-solute solution,
b) in mixed-solute solution

Adsorption Kinetics

In order to define the adsorption kinetics of HANs the kinetic parameters for the adsorption process were studied for contact times ranging from 1 to 90 min. The data were then regressed against a first-order kinetics equation and against a pseudo-second-order kinetics equation. Comparison between the experimental adsorption data and the theoretical values are illustrated in Figs. 5 and 6 and the results are listed in **Table 2**.

The theoretical q_e values for second-order kinetic models were higher than of pseudo-first order kinetic models and the correlation coefficients were higher also showing that adsorption of HANs on to the adsorbent obeyed second-order kinetic model.

Consistent with this notion is that Wu et al. reported that the pseudo-second-order model was suitable to explain the adsorption of low molecular weight compounds on small adsorbent particles. Also the initial adsorption rate on O-MWCNTs is high.

The intraparticle diffusion model proposed by Weber and Morris was adopted to verify the mechanism controlling the HANs adsorption process. Generally, the adsorption process over any porous adsorbent involves three consecutive mass transfer steps: film or external diffusion, pore diffusion and adsorption at the site on the adsorbent surface.

The data-fitting curves for intraparticle diffusion model are shown in **Fig. 8**. As can be seen, the q_t vs. $t^{0.5}$ relations for TCAN displays multi-linearity,

indicating that multiple adsorption steps are involved in the adsorption process.

The first regime represented the external mass transfer in the boundary layer while the second one was accounted for the diffusion of TCAN molecules through the pores of the adsorbent simultaneously with a gradual adsorption on the surface.

Finally, the horizontal line at longer time points illustrated attaining the adsorption equilibrium. In the case of DBAN, DCAN, MCAN and MBAN the external diffusion is not observed; the first linear regime can be reasonably correlated to the intraparticle diffusion. The adsorption of TCAN on O-MWCNTs showed at least two phases but did not plateau out.

This is consistent with the level of hydrophobicity of the TCAN molecule, where this property might increase the film resistance of water to mass transfer surrounding the adsorbent particle.

The rate constant of the first regime corresponds to the external mass transfer, where the larger the value the faster the external diffusion. The rate constant of this model are listed in **Table 3**, where it can be seen that the order of the rate constant was DBAN > DCAN >MCAN > MBAN > TCAN. For TCAN the intraparticle diffusion rate constant is determined from the slope of the second regime.

Isotherm Models

In order to model the adsorption mechanism, Langmuir and Freundlich isotherm models were used to test the experimentally adsorption process data for correlation. The results are plotted in Fig. 8. The best fitting for HANs adsorption on O-MWCNTs (**Table 4**), supported by the R^2 values for the two isotherms.

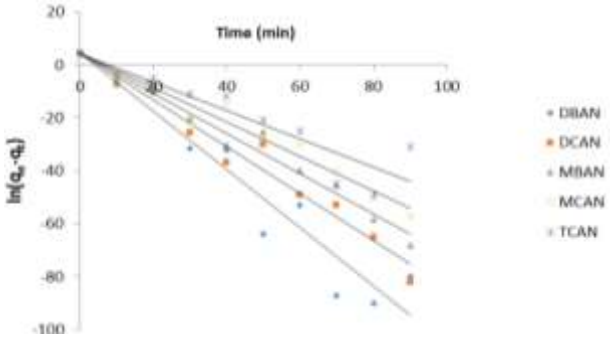

Fig. 6. Pseudo-first order adsorption kinetics of HANs onto O-MWCNTs adsorbent

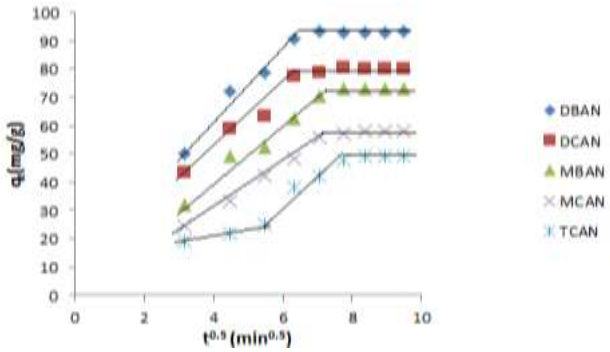

Fig. 7. Pseudo-second order adsorption kinetics of onto O-MWCNTs adsorbent

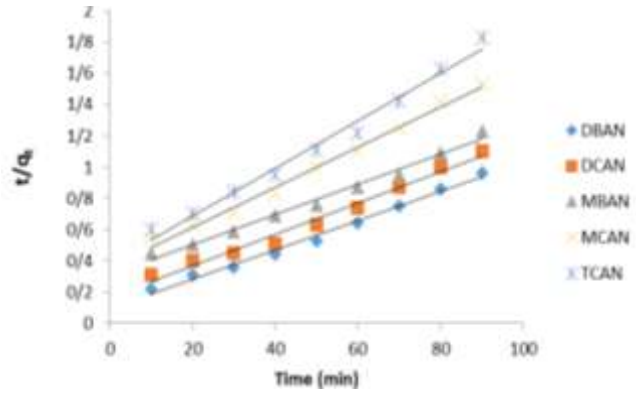

Fig. 8. Intraparticle diffusion model for the HANs adsorption O-MWCNTs.

Table 2. The first and second order kinetic constants of HANs adsorption

HAN	First-order kinetic			Second-order kinetic		
	q_e ($\mu g.g^{-1}$)	k_1 (min^{-1})	R^2	q_e ($\mu g.g^{-1}$)	k_2 ($g.\mu g^{-1}.min^{-1}$)	R^2
DBAN	93.2	1.1	0.92	107.2	1.12	0.99
DCAN	90.2	0.88	0.96	99.4	1.09	0.99
MBAN	91.3	0.76	0.96	102.2	0.94	0.98
MCAN	70.2	0.64	0.96	78.12	0.9	0.99
TCAN	56.4	0.53	0.83	65.3	0.87	0.97

Table 3. Kinetic parameters of HANs adsorption onto the O-MWCNTs adsorbent using the intraparticle diffusion model

HANs	K_{d1}	C_1	R^2	K_{d2}	C_2	R^2
DBAN	13.05	9.02	0.98			
DCAN	10.69	8.17	0.97			
MBAN	9.47	1.2	0.97			
MCAN	7.7	0.5	0.99			
TCAN	1.1	0.97	0.99	6.58	1.15	0.98

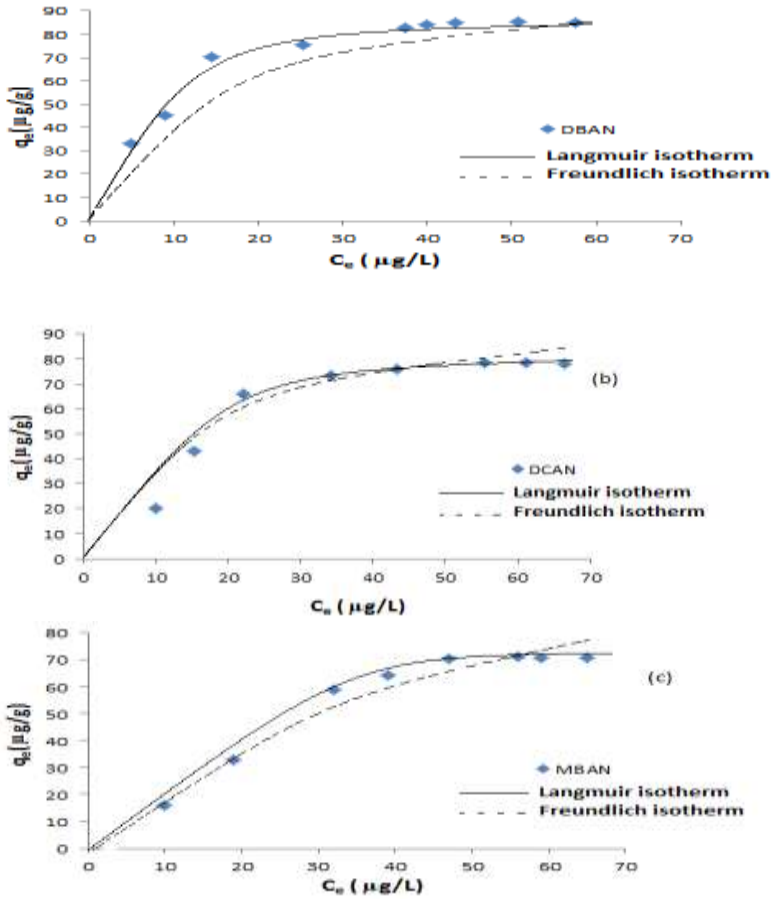

Fig. 9. Comparison of the predicted and experimental data for the equilibrium adsorption of five HANs on O-MWCNTs, (a) DBAN, (b)DCAN, (c) MBAN

Table 4. Isotherm parameters of HANs adsorption on O-MWCNTs adsorbent

	HANs				
Isotherms	DBAN	DCAN	MBAN	MCAN	TCAN
Langmuir					
q_m(μg g^{-1})	533.3	502.1	491.3	334.5	298.2
K_L (Lμg^{-1})	9.1	8.36	7.78	7.1	6.3
R^2	0.99	0.98	0.99	0.98	0.97
Frendlich					
1/n	0.65	0.49	0.48	0.45	0.42
K_F(μg g^{-1})	620.2	631.2	602.3	600.3	593.3
R^2	0.78	0.83	0.85	0.89	0.93

As can be seen, the exponent 1/n value for HANs on O-MWCNTs was fairly close to unity, which means that the form of the HANs adsorption equilibrium on O-MWCNTs was more Langmuir like than Freundlich. So the adsorption of HANs molecules occurs on a homogenous surface by monolayer adsorption without any interaction between adsorbed particles.

Effect of O-MWCNTs pretreatment on PBS Membrane Flux

In this study, the influences of the O-MWCNTs pretreatment on the permeation flux and rejection of HANs is shown in **Fig. 10**. As can be seen, the permeate flux of PBS membrane reduces drastically with the time, which is rapid during the first 5 min and then follow by a more gradual decline to become constant. This behavior refers to concentration polarization and fouling of the membranes. Obviously, the permeation flux increases with usage of O-MWCNTs. It is might be related to the nature of the moderate hydrophilic HANs (except TCAN). On the other hand, O-MWCNTs particles selectively adsorbed hydrophilic organic matter, so the hydrophilic interaction between the O-MWCNTs particles and HANs molecules increasing. In contrast, the surface of PBS membrane is hydrophobic (contact angle: 76°), Therefore hydrophobic adsorption between waste water and PBS membrane is reduced and then consequently cannot result in membrane fouling. The membrane/adsorption configuration that was introduced in this study could adsorb the HANs and reduce the costs associated with fouling in membrane unit.

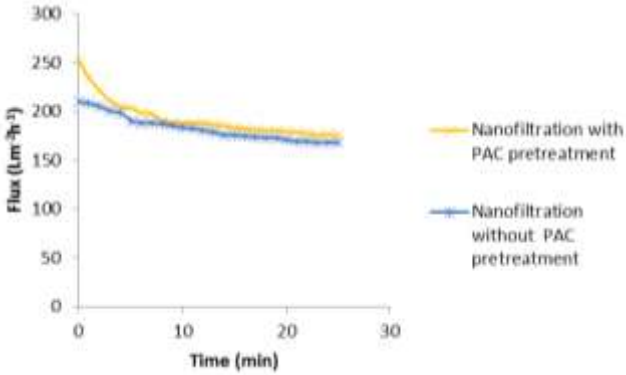

Fig. 10. Effect of O-MWCNTs pretreatment on PBS Membrane Flux

DOC and UV254 Removal Efficiencies of O-MWCNTs and NF Process

After water sample adsorbed by O-MWCNTs passing through NF membrane, the efficiencies of DOC and UV_{254} are shown in Fig. 10. From the figure, O-MWCNTs has a high removal rate of DOC. During O-MWCNTs dosage of 10–150 mg/L, DOC removal rate increased from 2.0% to 55.3%. When the NF membrane filtrated the water sample after O-MWCNTs adsorption, DOC removal of permeate increased steadily from 19.1% to 98.2%. However, DOC removal by NF membrane increased slightly with the increase of O-MWCNTs dosage. Compared to DOC, a high removal rate of UV_{254} was obtained. The UV absorbance removal increased from 10.5% to 71.2% with the

increment of O-MWCNTs dosage from 10 mg/L to 150 mg/L. Similar to the removal rate of DOC after NF filtration, at higher O-MWCNTs dosage, the higher the UV_{254} removal by the NF membrane was obtained (87/6%). It is likely that O-MWCNTs obtained a high removal of DOC and UV_{254} with high O-MWCNTs dosage (150 mg) and few residual organic matters that can be removed by the membrane.

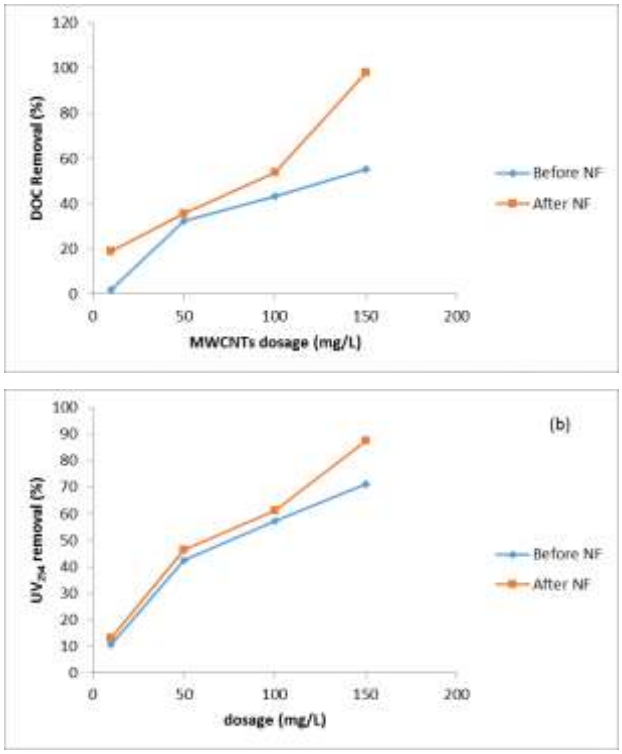

Fig. 11. DOC and UV_{254} Removal efficiencies of O-MWCNTs /NF Process

CONCLUSION

HANs removal from aqueous solution was investigated by a O-MWCNTs adsorption/ PBS membrane hybrid process. HANs adsorption on O-MWCNTs adsorbents followed a pseudo-second order rate kinetics model and the Langmuir isotherm can predict the equilibrium adsorption of five HANs on O-MWCNTs. In addition, DCAN adsorption is highly pH dependent, being favored at a high pH due to having a higher negative surface charge density. O-MWCNTs are used as pretreatment of NF membrane process in order to remove HANs and reduce membrane fouling. O-MWCNTs improved membrane flux slightly from 210 to 253 $Lm^{-2}h^{-1}$. O-MWCNTs offers higher DOC and UV254 removal rates on hybrid process. During 10–150 mg/L O-MWCNTs dosage at hybrid process, DOC removal rate of 19.1%-98.2% and UV254 removal rate up to 87.6% were obtained.

ACKNOWLEDGEMENTS

The study presented in this paper is part of a research project of Mohsen Vaziri (Department of Chemical Engineering, Mahshahr Branch, Islamic Azad University, Mahshahr, Iran).

Declaration of Competing Interest

The authors declared that they have no conflicts of interest to this work.

FUNDING

The authors gratefully acknowledge the Islamic Azad University of Kerman for financial supports.

DISCLOSURE STATEMENT

The authors reported no potential conflict of interest.

REFERENCES

[1]. A. Samimi, S. Zarinabadi, A. Bozorgian, A. Amosoltani, M. Tarkesh, K. Kavousi, Advances of Membrane Technology in Acid Gas Removal in Industries, *Progress in Chemical and Biochemical Research*, 3 (1) (2020), 46-54

[2] J.C. Lipscomb, E. El-Demerdash, A.E. Ahmed, Haloacetonitriles: metabolism and toxicity, Rev Environ Contam Toxicol 198 (2009), 169-200

[3] K. Yaowalak, P. Patiparn, W. Aunnop, Removal of haloacetonitrile by adsorption on thiol-functionalized mesoporous composites based on natural rubber and hexagonal mesoporous silica, Environ. Eng. Res 20 (2015), 342-346

[4] P. Panida, N. Chawalit, K. Sutha, P. Patiparn, Adsorption characteristics of haloacetonitriles on functionalized silica-based porous materials in aqueous solution, Journal of Hazardous Materials 192 (2011), 1210– 1218

[5] H.H. Tung, R.F. Unz, Y.F. Xie, HAA removal by GAC adsorption, J. Am. Water Works Assoc 98 (2006), 107–112

[6]. A. Samimi, S. Zarinabadi, M. Setoudeh, Safety and Inspection for Preventing Fouling in Oil Exchangers, *International Journal of Basic and Applied Sciences*, 1(2) (2012), 429-434

[7] C. Ratasuk, C. Kositanont, C. Ratanatamskul, Removal of haloacetic acids by ozone and biologically active carbon, J. Sci. Soc. Thai 34 (2008), 293–298

[8] K.G. Babi, K.M. Koumenides, A.D. Nikolaou, C.A. Makri, F.K. Tzoumerkas, T.D. Lekkas, Pilot study of the removal of THMs, HAAs and DOC from drinking water by GAC adsorption, Desalination 210 (2007), 215–224

[9] W. Zongping, D. Jiaqi, X. Pengchao, C. Yiqun, W. Songlin, Formation of halogenated by-products during chemical cleaning of humic acid-fouled UF membrane by sodium hypochlorite solution, Chem. Eng. J 332 (2018), 76-84

[10] J. Kim, B. Kang, (2008) DBPs removal in GAC filter-adsorber, Water Res 42 (2008), 145–152

[11] V. Uyak, I. Koyuncu, I. Oktem, M. Cakmakci, I. Toroz, Removal of trihalomethanes from drinking water by nanofiltration membranes, J. Hazard. Mater 152 (2008) 789–794

[12] S. Irene, R.D.S. Puche, S. Eloy, D. Prats, Reduction of chlorination byproducts in surface water using ceramic nanofiltration membranes, Desalination, 277 (2011), 147-155

[13] K.Y. Park, S. Choi, S.H. Lee, J.H. Kweon, J. Song, Comparison of formation of *disinfection* by-*products* by chlorination and *ozonation* of wastewater effluents and their toxicity to Daphnia magna, Environ Pollut 215 (2016), 314-321

[14] P. Deeudomwongsa, S. Phattarapattamawong, K. Lin, Control of disinfection byproducts (DBPs) by ozonation and peroxone process: Role of chloride on removal of DBP precursors, Chemosphere, 184 (2017), 1215-1222

[15] Y. Mao, X. Wang, H. Yang, H. Wang, Y.F. Xie, Effects of ozonation on disinfection byproduct formation and speciation during subsequent chlorination, Chemosphere, 117 (2014), 515-520

[16] S. Vigneswaran, W.S. Guo, P. Smith, H.H. Ngo, Submerged membrane adsorption hybrid system (SMAHS): process control and optimization of operating parameters. Desalination, 202 (2007), 392–399

[17] S.M. Tabatabaee Ghomshe, cleaning strategy of fouled reverse osmosis membrane: Direct osmosis at high salinities (DO-HS) as on-line technique without interruption of RO operation, Bulgarian Chemical Communications, 48 (2016), 57 – 64.

[18] C. Bellona, J.E. Drewes, Viability of a low-pressure nanofilter in treating recycled water for water reuse applications: a pilot-scale study, Water research, 41 (2007), 3948-3958

[19] T. Tanakaa, M. Takahashia, S. Kawaguchia, T. Hashimotoa, H. Saitoha, T. Kouyaa, M. Taniguchia, D.R. Lloydb, Formation of microporous membranes of poly (1,4-butylene succinate) via nonsolvent and thermally induced phase separation, Desalination Water Treat, 17 (2010), 176–182

[20] V. Ghaffarian, S.M. Mousavi, M. Bahreini, M. Afifi, Preparation and Characterization of Biodegradable Blend Membranes of PBS/CA, J Polym Environ, 21 (2013), 1150–1157

HOW TO CITE THIS ARTICLE

Mohsen Vaziri, Seyed Mostafa Tabatabaee Ghomsheh, Alireza Azimi, Masoumeh Mirzaei, Disinfection by-Products Removal Evaluation from Aqueous Solution by Hybrid Filtration Process, Prog. Chem. Biochem. Res., 3(4) (2020) 366-376.

DOI: 10.22034/pcbr.2020.113923
URL: http://www.pcbiochemres.com/article_113923.html